

ADVANCED MODELLING TECHNIQUES for AEROSPACE SMEs

DELIVERABLE 8.2: “SIMULATION OF THE LHP PROTOTYPE IN THE THERMAL CHAMBER (GROUND TEST)”

| | |
|---|-----------|
| NOMENCLATURE | 2 |
| 1 INTRODUCTION | 3 |
| 1.1 <i>Pressure drop & tabular (SINDA/FLUINT) connector</i> | 3 |
| 1.2 <i>Condensation & Flow pattern</i> | 7 |
| 1.3 <i>Results</i> | 9 |
| REFERENCES | 12 |

NOMENCLATURE

| <i>Variable</i> | <i>Description</i> |
|-------------------------|--|
| f_{TP} | Two-phase friction factor |
| Fr | Froude number |
| G [kg/m ² s] | Mass velocity |
| Ga | Galileo number |
| Ja | Jacob number |
| \dot{m} [kg/s] | Flow rate |
| P | Perimeter of the pipe |
| Pr | Prandtl number |
| Q [m ³ /s] | Volumetric velocity |
| Re | Reynolds number |
| S | Slip factor |
| u (m/s) | Velocity |
| V [m ³ /kg] | Specific volume |
| X | Mass vapour quality |
| X _{tt} | Martinelli parameter for turbulent flow in both phases |

Greek

| <i>Variable</i> | <i>Description</i> |
|-----------------------------|--|
| α | void fraction |
| ρ [kg/m ³] | fluid density |
| ϑ | Angle to horizontal plane |
| ϕ_{lo} | Two-phase frictional multiplier based on pressure gradient for liquid part of the total flow |
| τ | Shear forces |

Subscripts

| <i>Variable</i> | <i>Description</i> |
|-----------------|--------------------|
| V | Vapour |
| L | Liquid |

1 INTRODUCTION

Although the Alpha Magnetic Spectrometer (AMS) operational life is carried out in orbit under microgravity conditions, it is desirable to understand its behaviour also under gravity conditions since the AMS undergoes extensive ground testing (1 g) before launch to ensure that all the components are properly working. In particular, the thermal chamber has been designed to provide the ground experimental test (EM) of the propylene LHP system for the Alpha Magnetic Spectrometer. At this moment the thermal chamber experiment, forecast at the Shandong University in China, has been cancelled, consequently the comparison between the model and the real experimental ground test will not be carried out. Nevertheless the simulation of the propylene LHP in gravity condition has been done also for future uses in similar conditions.

In this deliverable a specific “gravity model” is introduced in the lumped parameter simulations and the results are then compared with the microgravity model (described in the deliverable 8.1) in order to test the portability of future ground tests to space conditions. In the 1G network the physical scheme includes pressure drop and heat transfer correlations. Moreover the fluid line is subdivided into two paths in order to let the liquid and the vapour flow separately as described in the separated flow model [1]. In this approach the two phases of the flow are considered to be artificially segregated. Two sets of basic equations can now be written, one for each phases. The two phases have different velocity as specified by a slip flow model. These information are explained in the next paragraph (1.1) while the heat transfer correlations are described in the 1.2. Finally the gravity model is compared with the microgravity results in the paragraph 1.3.

1.1 Pressure drop & tabular (SINDA/FLUINT) connector

In the microgravity model the two-phase flow is included in the same path. By using a single path to model a channel where a two-phase fluid is flowing, the user is implicitly assuming that the flow is homogeneous, meaning that the velocities of each phase are equal. In fact, for most purposes a two-phase fluid flow is modelled as a single effective phase having properties intermediate between pure liquid and pure vapour phases.

This assumption is usually adequate for reduced gravity and is both simple to implement and fast to execute. Because of such an assumption, there is no difference between the flow quality and thermodynamic quality: *thermodynamic quality* is the fraction of vapour mass within a segment of the pipe divided by the total mass in that segment: $M_v/(M_v+M_l)$. *Flow quality* is the ratio of vapour mass flow rate through a segment divided by the total mass flow rate through that segment: $m_v/(m_v+m_l)$.

In reality, vapour usually moves faster than liquid, and sometimes even in opposite directions. In addition gravity is a crucial parameter in a two-phase flow [2]. When its effect is included in the model the buoyancy force exerted due of the difference in density between the gas and the liquid has a major impact on the flow regime and the distribution of void fraction. A so-called slip flow formulation is then considered, using one momentum equation per phase and letting the bulk velocities of the liquid and the vapour being different along the LHP lines. Therefore, the fluid line in the gravity model has been modelled by using two paths to let the liquid and the vapor to flow separately (Fig. 1.1).

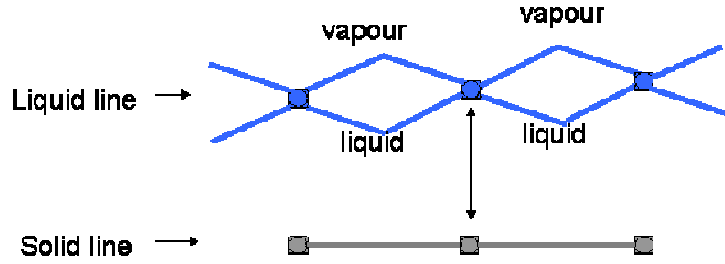


Fig. 1.1. Tabular connectors for the LHP model

Unlike homogeneous flow, adding a slip flow the thermodynamic quality is no longer the same as the flow quality. Conservation of mass dictates that flow quality must be the same (eventually) whether a homogeneous or slip flow formulation is used. However, the thermodynamic quality is no longer constrained by the homogeneous assumption: it becomes the new degree of freedom necessary to accommodate a new momentum equation. In other words, the thermodynamic quality and its manifestations, such as the density and void fraction, will vary as needed to balance the flow forces. Because vapor generally travels faster than liquid, the void fraction will be smaller with slip flow than with homogeneous flow at the same flow quality. In other words, more liquid will reside in the line, and the thermodynamic quality will be smaller than the flow quality.

The separation of the line of liquid and the vapour line is resembling the common “two-phase model” in two-phase flow model. The pressure drop (along the linear coordinate z) is related to the friction head, the acceleration head and the static head [1]:

$$\begin{aligned}
 & \text{Friction head} \qquad \qquad \qquad \text{acceleration head} \\
 -\left(\frac{dp}{dz}\right) = & \frac{\frac{2f_{TP}G^2v_l}{D}\phi_{lo}^2 + G^2 \frac{dx}{dz} \left[\left\{ \frac{2xv_v}{\alpha} - \frac{2(1-x)v_v}{(1-\alpha)} \right\} + \left(\frac{\partial\alpha}{\partial x}\right)_p \left\{ \frac{(1-x)^2v_l}{(1-\alpha)^2} - \frac{x^2v_v}{\alpha^2} \right\} \right]}{1 + G^2 \left[\frac{x^2}{\alpha} \left(\frac{dv_v}{dp}\right) + \left(\frac{\partial\alpha}{\partial p}\right)_x \left\{ \frac{(1-x)^2v_l}{(1-\alpha)^2} - \frac{x^2v_v}{\alpha^2} \right\} \right]} + \qquad 1.1 \\
 & \underbrace{g \sin \vartheta [\rho_v \alpha + \rho_l (1-\alpha)]}_{\text{static head}}
 \end{aligned}$$

A particular SINDA/FLUINT tool, called *tabular* connector, is used to account for the 3 components (friction, acceleration, static head). The *Tabular* connector allows users to specify flow rate (m) versus head (H) relationships in tabular (array) formats:

$$H = C_0 + C_1 \dot{m} + C_2 \dot{m}^2 \qquad 1.2$$

An assumption of symmetry is made by default: $H(m)$ for positive m is applied as $-H(m)$ if m is negative. This allows the user to define one equation, cast in the form of (1.2), that applies in both directions if there is no difference between forward and reverse flows. Alternatively, if the device is “directional” (i.e., it behaves differently if flow rates reverse), then the user can

supply a more complete equation that include the negative flow rate regions. Fig. 2.2 provides an illustration of these two options.

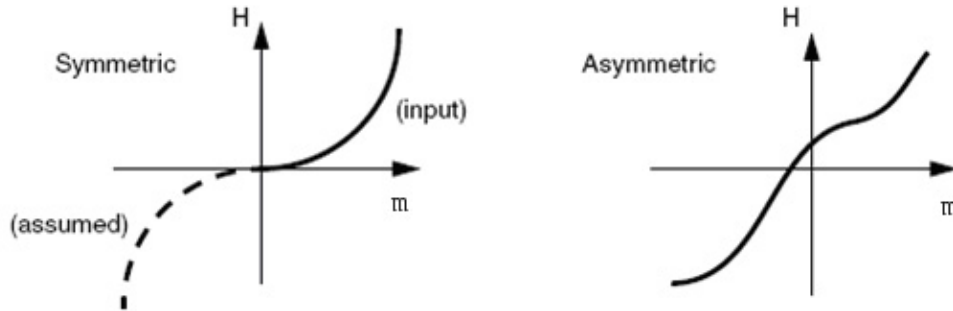


Fig. 1.2. Graphical Examples of Symmetric and Asymmetric Head-Flow rate Curves

The relationship (1.2) is set for two connectors flowing parallel and simulating the liquid and the vapour part of the two-phase flow, and it is used for the liquid, vapour and condenser line in the SINDA model.

To reproduce the pressure drop achieved by a separated two-phase flow we have to consider equation (1.1) modified in order to be implemented in the network-style simulator. Since the fluid volume inside the vapour, liquid and condenser lines is small compared with the fluid in the compensation chamber the flow rate variations are damped and hence it is possible to use a steady state equation:

$$\underbrace{A dp - \tau_v P_v dz - \tau_l P_l dz}_{\text{Shear forces}} - \underbrace{g \sin \vartheta [A_v \rho_v + A_l \rho_l]}_{\text{Gravitational forces}} = \underbrace{d(\dot{m}_v u_v + \dot{m}_l u_l)}_{\text{Acceleration forces}} \quad 1.3$$

The gravity term is:

$$g \sin \vartheta [(1 - \alpha) \rho_l + \alpha \rho_g] \quad 1.4$$

and the friction forces:

$$\tau_v P_v + \tau_l P_l = A \left(\frac{dp}{dz} \right)_F \quad 1.5$$

Where A is the area of the pipe. The friction pressure drop is calculated by the Muller-Steinhagen and Heck method. The Muller-Steinhagen & Heck [4] correlation predicts the two-phase pressure drop in a straight tube based on the pressure drops of liquid and vapour phases, which are calculated separately:

$$\left. \frac{dp}{dz} \right|_k = 2 \frac{f_k G^2}{D \rho_k} \quad 1.6$$

Where $f_k = 0.079 \text{Re}_k^{-0.25}$, D is the diameter of the pipe and k represents either vapour (v) or liquid (l). The pressure drops computed for each phase are then combined:

$$\left(\frac{dp}{dz}\right)_F = \left[\frac{dp}{dz}\Big|_l + 2x \left(\frac{dp}{dz}\Big|_v - \frac{dp}{dz}\Big|_l \right) \right] (1-x)^{1/3} + \frac{dp}{dz}\Big|_v x^3 \quad 1.7$$

By inserting eq. (1.6) and (1.7) in the (1.4):

$$\tau_v P_v + \tau_l P_l = \left\{ \frac{2}{A \cdot D} \left[\frac{f_l}{\rho_l} + 2x \left(\frac{f_v}{\rho_v} - \frac{f_l}{\rho_l} \right) \right] (1-x)^{1/3} + 2 \frac{f_v}{D \rho_v} x^3 \right\} \dot{m}^2 = f_{MH} \dot{m}^2 \quad 1.8$$

Where f_{MH} is a factor that includes the Muller-Steinhagen & Heck correlation.

Tribbe and Muller-Steinhagen [4] have shown that the Muller-Steinhagen and Heck method gave the best results in a comparison of competing methods to a large experimental database that covered flows of air-oil, air-water, water-steam and several refrigerants, applicable for $0 \leq x \leq 1$. Moreover this method provides a fast estimation and a smooth transition between the single phase and the two-phase mode.

Finally, the acceleration forces are implemented using an acceleration factor (AC):

$$d(\dot{m}_l u_l + \dot{m}_v u_v) = AC \dot{m}^2 \quad 1.9$$

Where \dot{m} is the overall flow rate.

The AC is related to the density changes between two sections of the pipe (1 and 2) by the equation [6]:

$$AC = \frac{2(\rho_2 - \rho_1)}{\rho_1 \rho_2 A^2} \quad 1.10$$

In the equation (1.2) the coefficient are then defined as:

$$C_0 = g \sin \vartheta [(1-\alpha)\rho_f + \alpha \rho_g] \quad 1.11$$

$$C_1 = 0$$

$$C_2 = [f_{MH} + AC]$$

By eq. 1.11 and 1.2 the pressure drop can be defined in the gravity model as a function of the mass flow rate both for the liquid and for the vapour path. In the following simulations the LHP is considered to be plane ($\vartheta = 0$) so that all the model nodes have the same elevation and, consequently the C_0 is zero:

$$C_0 = 0 \quad 1.12$$

$$C_{2,l} \dot{m}_l^2 = C_{2,v} \dot{m}_v^2$$

Where $C_{2,l}$ and $C_{2,v}$ are the factors for the liquid and the vapour respectively. The latter can be implemented to account for the slip flow between the phases ($S=u_v/u_l$):

$$\frac{C_{2,l}}{C_{2,v}} = \frac{\rho_l^2}{\rho_v^2} \frac{1}{S^2} \quad 1.13$$

Several of the available slip models can be cast in the general form [3]:

$$S = C \left(\frac{1-x}{x} \right)^{p-1} \left(\frac{\rho_v}{\rho_l} \right)^{q-1} \left(\frac{\mu_l}{\mu_v} \right)^r \quad 1.14$$

The values of constants (C, p q and r) corresponding to the different models are listed in the Table below.

| Model | C | p | q | r |
|----------------------------------|------|------|------|------|
| Lockhart & Martinelli (1949) | 0.28 | 0.64 | 0.36 | 0.07 |
| Fauske (1962) | 1 | 1 | 1/2 | 0 |
| Thom (1964) | 1 | 1 | 0.89 | 0.18 |
| Zivi (1964) | 1 | 1 | 0.67 | 0 |
| Baroczy (1965) | 1 | 0.74 | 0.65 | 0.13 |
| Moody (1965) | 1 | 1 | 2/3 | 0 |
| Wallis (1969) separated-cylinder | 1 | 0.72 | 0.40 | 0.08 |
| Homogeneous (Wallis, 1969) | 1 | 1 | 1 | 0 |

Table 1.1 Models for predicting the slip ratio. The constants C, p, q and r come from the model implemented

The fluid properties of the tubular connector are averaged between the two lump nodes at the ends. A “released factor” to smooth the property changes as well as a maximum ratio for the slip flow are implemented to avoid not physical oscillations of these values.

1.2 Condensation & Flow pattern

When the LHPs run under a gravity environment the so-called Dobson and Chato method is implemented [4]. They proposed a calculation scheme which includes both a stratified-wavy flow method with film condensation from the top towards the bottom of the tube and an annular flow correlation.

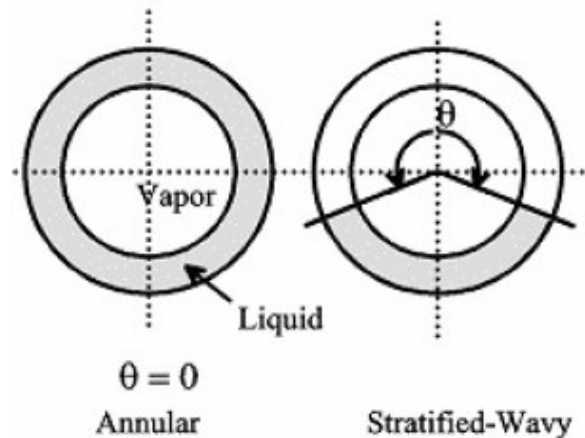


Fig. 1.3. Simplified flow structures for annular and stratified-wavy regimes

Their annular flow condensation correlation is:

$$Nu = 0.023 \cdot Re_{Ls}^{0.8} Pr_L^{0.4} \left[1 + \frac{2.22}{X_{tt}^{0.89}} \right] \quad 2.15$$

Where Re_{Ls} is the superficial Reynolds number given by the superficial velocity V_{SL} (defined as the rate of volumetric flow divided by the flow area, Q/A), and X_{tt} is the Martinelli parameter for turbulent flow in both phases:

$$X_{tt} = \left(\frac{1-x}{x} \right)^{0.9} \left(\frac{\rho_v}{\rho_l} \right)^{0.5} \left(\frac{\mu_l}{\mu_v} \right)^{0.1} \quad 2.16$$

To implement the method for stratified-wavy flow, first the void fraction α is calculated using the Zivi void fraction:

$$\alpha = \frac{1}{1 + [(1-x)/x](\rho_v/\rho_l)^{2/3}} \quad 2.17$$

Assuming all the liquid is stratified in the bottom of the tube (neglecting condensate formed on the walls and considering a horizontal tube), the angle from the top of the tube to the stratified liquid layer in the bottom θ_{strat} is then determined (with a numerical approximation) as:

$$1 - \frac{\theta_{strat}}{\pi} \cong \frac{\arccos(2\alpha - 1)}{\pi} \quad 2.18$$

The stratified-wavy heat transfer coefficient is obtained by a protraction between the film condensation coefficient on the top perimeter of the tube (left term) and the forced convective heat transfer coefficient on the stratified perimeter (right term) as:

$$Nu = \frac{0.23 Re_{Go}^{0.12}}{1 + 1.11 X_{tt}^{0.58}} \left[\frac{Ga_L Pr_L}{Ja_L} \right]^{0.25} + (1 - \theta_{strat} / \pi) Nu_{strat} \quad 2.19$$

where Ga_L is the liquid Galileo number, Ja_L the liquid Jacob number
Forced convection condensation in the stratified liquid is correlated as:

$$Nu_{strat} = 0.0195 Re_{Ls}^{0.8} Pr_L^{0.4} \left(1.376 + \frac{c_1}{X_{tt}^{c_2}} \right)^{1/2} \quad 2.20$$

The empirical constants c_1 and c_2 are obtained as a function of the Froude number Fr_L as follows:

For $0 < Fr_L \leq 0.7$:

$$c_1 = 4.172 + 5.48Fr_L - 1.564Fr_L^2$$

$$c_2 = 1.773 - 0.169Fr_L$$

For $Fr_L > 0.7$:

$$c_1 = 7.242$$

$$c_2 = 1.655$$

As specified by the Dobson and Chato method, the Soliman transition criterion for predicting the transition from annular flow to stratified-wavy flow was used to distinguish which heat transfer regime is to apply. The method is based on a Froude transition number Fr_{so} given as:

$$Fr_{so} = 0.025 \cdot Re_{Ls}^{1.59} \left(\frac{1 + 1.09X_{tt}^{0.039}}{X_{tt}} \right)^{1.5} \frac{1}{Ga_L^{0.5}} \quad \text{with } Re_{Ls} \leq 1250 \quad 1.21$$

$$Fr_{so} = 1.26 \cdot Re_{Ls}^{1.04} \left(\frac{1 + 1.09X_{tt}^{0.039}}{X_{tt}} \right)^{1.5} \frac{1}{Ga_L^{0.5}} \quad \text{with } Re_{Ls} > 1250 \quad 1.22$$

While Soliman sets the transition from annular flow to wavy flow at $Fr_{so} = 7$, Dobson and Chato noted that a transition value of $Fr_{so} = 20$ fits their data better. Their method is then implemented as follows (Table 2.2):

- For mass velocities greater than 500 kg/m²s, the annular flow correlation [2.12] is always used;
- For mass velocities less than 500 kg/m²s, the annular flow correlation [2.12] is used when $Fr_{so} > 20$;
- For mass velocities less than 500 kg/m²s and for $Fr_{so} < 20$, the stratified-wavy correlation [2.15] is used;

| | FROUDE | G [Kg/m ² s] |
|-----------------|--------|-------------------------|
| ANNULAR | >20 | < 500 |
| ANNULAR | - | > 500 |
| STRATIFIED-WAVY | <20 | < 500 |

Table 1.2

1.3 Results

The comparison between the simulations in microgravity (μG) and gravity (1G) environment under the steady state mode may give us information about the feasibility of the LHP ground test to the space conditions. The compensation chamber (T_{CC}) and the subcooling temperatures (T_s) (the temperature outcoming from the radiator) are the most meaningful data for the LHP working, hence the influence of the gravity will be tested by analyzing their values. The boundary conditions used for this analysis are median between the hottest and the coldest environment: beta angle equal to zero and MPA attitude (the 11° case in the Figure 8 of the previous report [5]).

The next picture shows the results achieved from the gravity and the microgravity SINDA models: the T_{CC} and the T_S are depicted depending on the power inlet to the evaporator (Q).

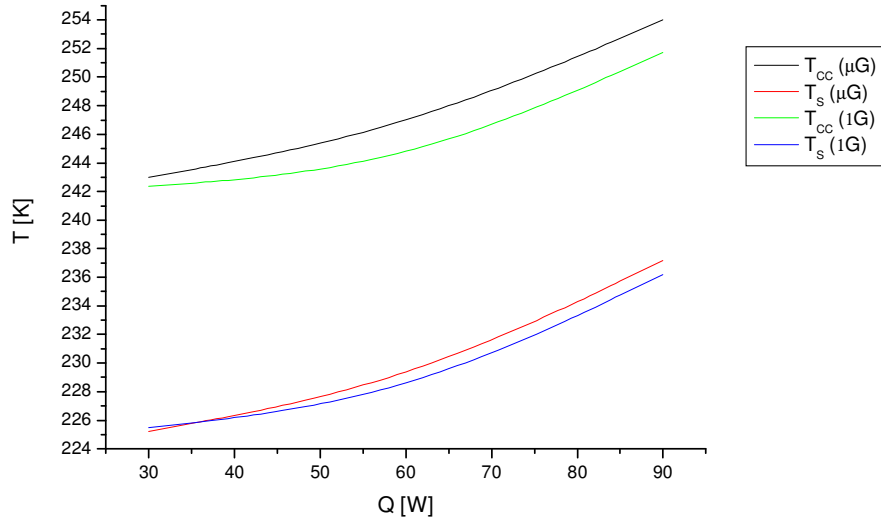


Fig. 1.4. Gravity and microgravity temperatures

The maximum difference (about 2 Kelvin) is for the compensation chamber temperatures with the maximum Q (90W). The reason of such difference may be either the pressure drop and the heat transfer correlations because they are differently implemented in the two models. The influence of the pressure drop can be achieved by analyzing the Clausius-Clapeyron correlation in the two-phase part of the condenser (two-phase length):

$$\Delta T = \frac{T v_{g-f}}{h_{fg}} \Delta P \quad 1.23$$

Because the gravity and the microgravity SINDA models implement two different kind of pressure drop scheme for the two-phase flow, the resulting ΔP in the two-phase length is different. By inserting the values achieved by the two models in equation (1.23) the temperature drop dues to the pressure drop is calculated. The next table show the results.

| | | MICROGRAVITY | | NORMAL GRAVITY | |
|---------|----|--------------|-----------------|----------------|-----------------|
| | | ΔT | ΔP (Pa) | ΔT | ΔP (Pa) |
| Q [W] | 30 | 0.008 | 69.3 | 0.012 | 97.2 |
| | 60 | 0.076 | 701.7 | 0.095 | 874 |
| | 90 | 0.16 | 1815.7 | 0.16 | 1791 |

Table 1.3 Pressure drop influence on the temperatures

As it is evident the temperature difference is little related to the pressure drop: the maximum effect (for 90W) is 0.16K and correspond to a pressure drop equal to 1815.7 Pa for microgravity and 1791 Pa for gravity

The second reason of the temperature differences in Fig. 1.4 may be the heat transfer to the condenser: in the microgravity model the Shah condensation correlation is implemented, while under gravity conditions the Dobson and Chato method is used. The latter includes both

a stratified-wavy and an annular flow equation and the Soliman criterion was used for predicting the transition (Table 1.2).

The flow rates calculated by the SINDA model are $6.5E-05$ kg/s, $1.3E-04$ kg/s and $2E-04$ kg/s for Q equal to 30, 60 and 90W respectively . As it is evident in the table 2.2 these values are much lower than the critical one, that is 500kg/s, and hence they set the fluid always in the stratified-wavy regime. Viceversa the Froude number could have values higher than its critical one (20) as shown in the next graphic.

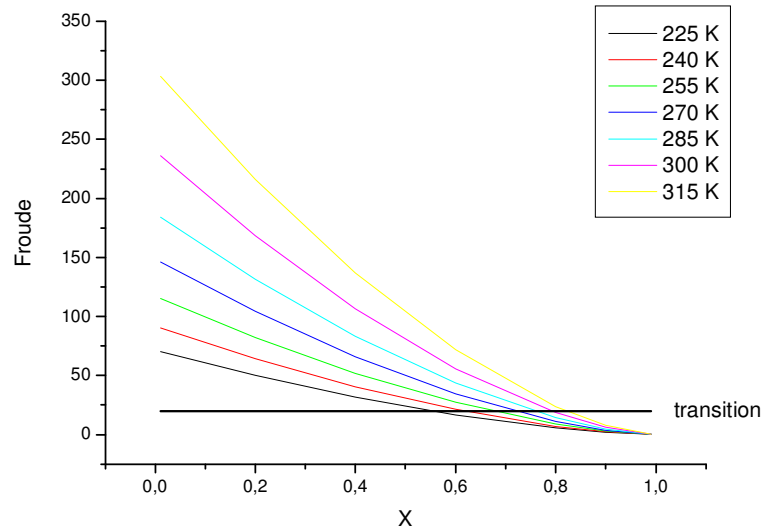


Fig. 1.5. Froude number for different temperature as a function of the quality

The transition from stratified-wavy to annular depends on the temperature and happens in the range between 0.6 and 0.8 of the flow quality. As a consequence of this transition the SINDA model use two different correlations during the run: the stratify-wavy correlation (Fig. 1.6 show the ratio between the Dobson & Chato stratify and the Shah) when the flow goes in the initial condenser section, and the annular equation (Fig. 1.7 show the ratio between the Dobson & Chato annular and the Shah) when x is reduced under about 0.7.

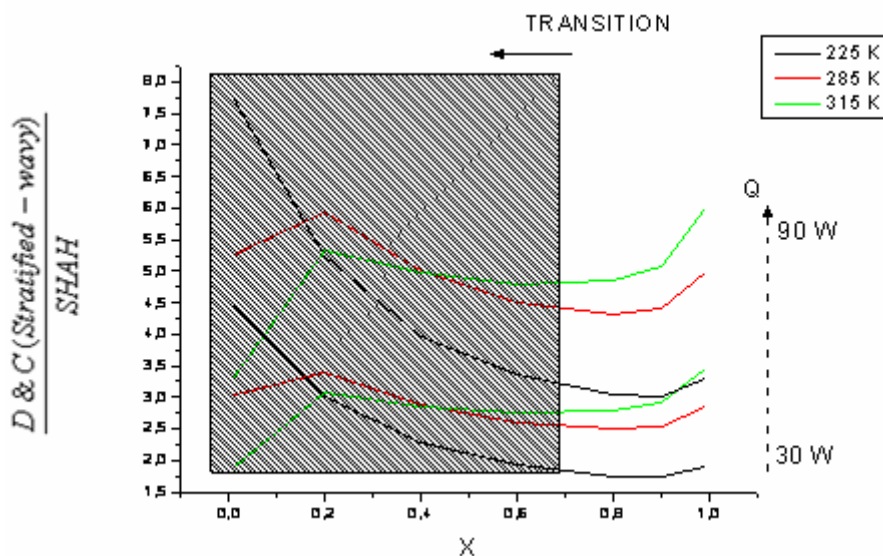


Fig. 1.6. Ratio between the Dobson & Chato stratify-wavy equation and the Shah correlation, The two correlations (and hence their ratio) depend on the temperature and on the quality

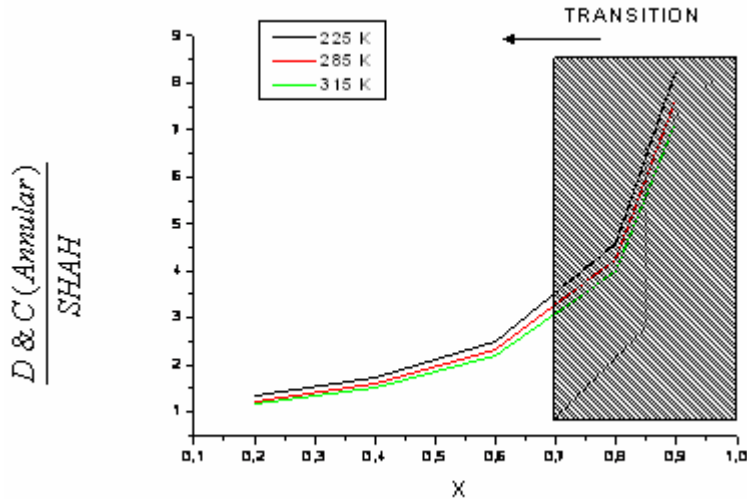


Fig. 1.7. Ratio between the Dobson & Chato annular equation and the Shah correlation, The two correlations (and hence their ratio) depend on the temperature and on the quality

In both cases the Dobson method has an heat transfer coefficient greater than the Shah equation. As a result a larger heat is rejected in the condenser and the outgoing temperature (=subcooling temperature) (and consequently the compensation chamber temperature) is lower (Fig. 1.4).

Moreover the difference between the two correlations increase while the power is increasing when the Dobson and Chato stratified method is considered (Fig. 1.6). This effect depends on two reasons: 1) Comparing the two equations it is clear a different relationship with the Reynolds number that is in turn connected to the flow mass evaporated in the evaporator and hence to the heat power. 2) the two phase length in the condenser section is longer when the power to reject is greater. In this case a major part of the condenser uses the condensation heat transfer method and consequently the difference between the gravity and the microgravity models is more evident.

REFERENCES

1. Collier, J. G., Thome, J. R. , Convective boiling and condensation. 3rd Ed., Oxford science publications.
2. R. Balasubramaniam, E. Ramé, J. Kizito, and M. Kassemi. Two Phase Flow Modeling: Summary of Flow Regimes and Pressure Drop Correlations in Reduced and Partial Gravity, National Center for Space Exploration Research, Cleveland, Ohio, NASA/CR—2006-214085
3. Quoc-Khanh Tran, 2002. Two-Phase Flashing Flow Slip Model For Slurry Flow Applications, *Applications of two-phase flashing*
4. John R. Thome, Wolverine Engineering Data Book III, 2006
5. Zinna S. & Marengo M. 2006 Simulation of the LHP in orbital conditions. *INTERREG IICMATEO-ANTASME Deliverable 8.1.*
6. C&R technologies, SINDA/FLUINT user's manual. March 2004, version 4.6